

Towards a 240 GHz Megawatt-class Gyrotron for Proxima Alpha

A. Schmidt¹, L. Feuerstein¹, S. Illy¹, J. Jelonnek¹, L. Milanese², J. Lion², M. Thumm¹, C. Wu¹

¹Institute for Pulsed Power and Microwave Technology (IHM), Karlsruhe Institute of Technology (KIT), Germany

²Proxima Fusion GmbH, Germany
andre.schmidt@kit.edu

Abstract—Karlsruhe Institute of Technology (KIT) is advancing the research and development of a short-pulse pre-prototype as the base for a continuous-wave (CW) industrial gyrotron with an output power exceeding 1 Megawatt (MW) at an operating frequency of around 240 GHz. It shall become the key component of an Electron Cyclotron Resonance Heating (ECRH) system for a future fusion power plant operating at a toroidal magnetic field of around 9 Tesla, specifically designed for Proxima Alpha. The pre-prototype shall be built-up and tested at the KIT FULGOR gyrotron test-facility, that will receive a 10.5 Tesla superconducting gyrotron magnet latest by 2025. This paper outlines the development for advancing the 240 GHz gyrotron. Possible designs are evaluated for their potential to manage the thermal loading, to minimize mode competition, and, to advance operating stability. The fundamental design choices and key challenges, including thermal management, cavity mode selection, and precision alignment, as well as simulation results for electron beam propagation and cavity performance are discussed.

Keywords—Nuclear fusion, Electron Cyclotron Resonance Heating, ECRH, gyrotron, coaxial-cavity technology, mode selection

I. INTRODUCTION

Today, gyrotron oscillators (gyrotrons) are the only microwave sources known that are capable to supply the necessary output power at the required frequencies, pulse lengths and efficiencies as required for Electron Cyclotron Resonance Heating (ECRH) systems of nuclear fusion experiments and future fusion power plants [1]. As the operating frequency of an ECRH system corresponds to the electron cyclotron frequency, the operating frequency is approximately by a factor of 28 GHz T^{-1} proportional to the magnetic field at the location of heating within the plasma. Hence, considering a toroidal magnetic field of approximately 9 T results in an operating frequency of minimum 240 GHz for the gyrotron. Proxima Alpha is a high field quasi-isodynamic stellarator that Proxima Fusion is currently designing to operate solely with ECRH at this frequency. One of the research focuses at KIT targets exactly for the development of next-generation gyrotrons to meet this demand. Additionally, the gyrotron shall deliver an output power above 1 MW at continuous waves.

Major result of the initial research and development is the fundamental decision for a conventional-type gyrotron design with a hollow circular waveguide cavity, or, alternatively, a more advanced coaxial-cavity gyrotron, which incorporates an

inner conductor. Coaxial-cavity gyrotrons offer key advantages such as a much reduced voltage depression and, potentially, decreased mode competition. That is visible particularly at higher operating frequencies and higher beam currents as required for operation above 1 MW. However, despite those benefits, the design and integration of the coaxial insert are significant challenges, considering the necessary precise mechanical alignment, efficient cooling, and possible vibrations during transport and operation. Therefore, it is essential to carefully evaluate the appropriate design choice before moving forward.

II. FUNDAMENTAL CONSIDERATIONS

This work starts from earlier hollow-cavity designs for Wendelstein 7-X (W7-X) [2], ITER [3] and the coaxial-cavity designs for the 170 GHz, 2 MW gyrotron [4] for DEMO [5]. To address the challenge of an operating frequency at 240 GHz, the obvious first step is to scale down the cavity size of the gyrotron to match the reduced wavelength. However, this increases the thermal loading of the cavity walls of the gyrotron, which poses a significant problem due to the limited capacity of existing cooling systems. To address this, the key components of the gyrotron must be redesigned to efficiently manage the increased thermal load and overcome the challenges that arise during the redesign process.

A. Maximum output power considering a maximum thermal loading

When scaling a gyrotron design to higher frequencies, the peak ohmic wall loading, ρ_{ohm} , increases proportionally to $f^{2.5}$. The cooling system implemented in conventional gyrotrons for W7-X and ITER can manage an ohmic loading of up to $\rho_{\text{ohm}} = 2 \text{ kW cm}^{-2}$ on the outer cavity wall during CW operation. According to [6] the maximum possible output power, can be estimated by

$$P_{\text{out}} = \frac{c^3 \sqrt{\mu_0} L}{2.8 \sqrt{\pi} \lambda} \sqrt{\sigma} \frac{(\chi^2 - m^2)}{Q} f^{-2.5} \rho_{\text{ohm}} \quad (1)$$

where c is the speed of light in vacuum, μ_0 is the vacuum permeability, σ is the electrical conductivity, L/λ is the cavity length in wavelength terms and Q is the quality factor of the cavity. The cavity electromagnetic (EM) field can be expanded in transverse electric modes ($\text{TE}_{m,n}$) with the eigenvalue χ (n^{th}

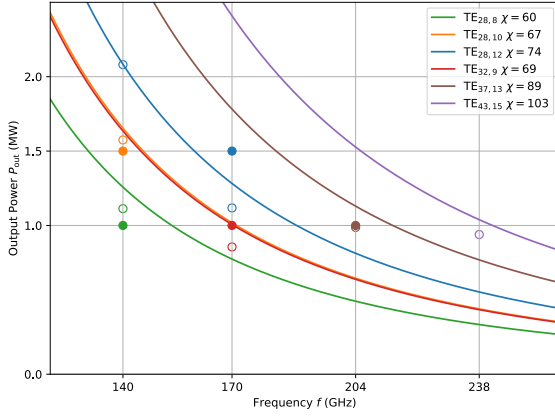


Fig. 1. Output power limitation by thermal load as a function of frequency for different operating modes. The simulation and approximation parameters are: $\rho_{\text{ohm}} = 2 \text{ kW cm}^{-2}$; $L/\lambda = 9$; $\sigma = 1.73 \times 10^7 \text{ S m}^{-1}$; $Q \approx 1400$.

root of the derivative of the Bessel function). This dependency arises from two factors: the skin depth, which scales as $\sim f^{0.5}$, and the ohmic quality factor, which scales as $\sim f^2$. It must be mentioned, that the equation 1 is derived from simplified assumptions, such as non-self-consistent simulation, a gaussian axial field profile and a mono-mode excitation. Nevertheless, the equation is a proper first estimate for power capabilities for different operating modes at specific operating frequencies.

The figure 1 shows the calculated output power limits at different frequencies for various proposed TE modes for gyrotron operation using the equation (1). The lines represent the estimated wall-loading limits. Simulated results are represented by hollow circles, which correspond to theoretical cavity designs created to hold the maximum ohmic loading criterion, while filled circles correspond to experimental data [2], [3], [7]–[9]. Notably, the blue data point for experimental data operates with a higher wall loading of 3 kW cm^{-2} [8] and the red data point has a shorter cavity with $L/\lambda < 8$ [3]. By utilizing a higher order mode, the cavity size can be increased and therefore the thermal load is reduced and the output power can be increased. As the figure demonstrates, the modes, currently utilized for operation are unsuitable for achieving output powers of 1 MW at about 240 GHz. Only the $\text{TE}_{43,15}$ mode, proposed in [10], may reach this threshold. However, with larger cavity radius and smaller wavelengths, the risk of mode competition increases, complicating efforts to maintain stable, high-power operation due to the excitation of unwanted modes.

B. Mode Competition

Mode competition arises when multiple modes are able to exchange energy with the electron beam. This results in a decreased efficiency, reduced achievable power, and operational stability. Because of the distribution of the roots of the Bessel functions and their derivatives, the number of possible propagating modes scales approximately with f^2 . The possible coupling range to the mode becomes smaller, making tolerance requirements stricter. Furthermore, backward waves, traveling in the opposite direction to the electron beam,

increase the problem by interfering with the intended forward modes, causing additional instability. Minimal tolerances, along with effective suppression techniques, are essential to mitigate these issues. [11]

C. Considering mechanics tolerances

The interaction between the electron beam and the EM field is highly dependent on the input parameters of the electron beam to the interaction region. To determine these parameters, it is important to analyze the beam path from the electron gun, the so-called Magnetron Injection Gun (MIG), to the cavity entrance. Achieving optimal performance in high-frequency gyrotrons requires maintaining a low velocity spread and minimizing the thickness of the electron beam. The initial characteristics of the annular electron beam are significantly influenced by the emitter geometry, including its radius, width, and slant angle, as well as the direction and strength of the electric and magnetic fields at the emitter location.

D. Fundamentals on the coaxial-cavity design

An option to reduce mode competition for a more stable operation is the usage of a coaxial insert. The insert, which extends into the interaction region of the cavity to form a coaxial waveguide, is supported only by a single attachment to the magnetron injection gun. Longitudinal impedance corrugations on the insert lead to an adjustment of the quality factors of modes with smaller caustic radii, than the operating mode. The insert thereby suppresses nearby competing modes, reducing mode competition and ensuring more stable and efficient operation. Another benefit is the lower voltage depression since the induced charge on the inner conductor reduces the total amount of space charge within the electron beam.

The coaxial insert must be precisely aligned with the magnetic field, the outer cavity wall and the electron beam. This alignment is critical during manufacturing, transport, and operation, as resonance-induced misalignment could cause permanent displacement. The insert should have a maximum possible radius to avoid excessive susceptibility to vibrations or other external influences and to facilitate water cooling. On the other hand, there has to be a safety distance to the electron beam, typically estimated by 20 times the larmor radius.

There are several conditions for the design of the inner conductor's corrugations. The depth of the corrugations should be approximately $d = \frac{\lambda}{4} \approx 0.3 \text{ mm}$. The number of corrugations N should be as high as possible for better mode suppression. At least $N = 2m$ is used; otherwise, azimuthal mode conversion must be accounted for. The minimal fabrication width a of the corrugations is assumed to be between 0.2 mm and 0.3 mm. Thus, the maximum number of corrugations is given by:

$$N = \pi \frac{r_{\text{insert}}}{a} \quad (2)$$

The number of corrugations should fall within these two limits. To confirm the effectiveness of the design approaches

with and without an insert, detailed simulations are essential. [12]

III. DESIGN AND SIMULATION

Addressing those challenges, the design of both the cavity and the MIG becomes critical in managing thermal loads, minimizing mode competition, and ensuring stable high-frequency operation. To verify proposed designs simulations with the program EURIDICE [13] for the beam-wave interaction in the cavity and ESRAY [14] for the MIG and the electron beam propagation have been used.

A. Cavity design

To evaluate their performance, both hollow- and coaxial-cavity designs are simulated, incorporating realistic spreads for the electron beam parameters. The start-up process involves gradually increasing the voltage, current, and pitch factor α (ratio of an electron's transverse to axial velocity relative to the magnetic field) over time. Ensuring that the correct mode is excited during start-up is crucial, as once a mode is established, the dominating one suppresses the others. For more realistic simulations the parameters used for the electron beam spreads in the simulation were: $\Delta\alpha = 6\%$, $\Delta v_{\text{beam}} = 1\%$, and $\Delta\gamma = 0.1\%$.

In the hollow-cavity simulation, a design capable of exciting the $\text{TE}_{43,15}$ mode, as proposed in [10] and referenced in II-A, was analyzed. Figure 2 illustrates the start-up process for this mode. The simulation results suggest that achieving a stable output power of 1 MW within wall loading constraints is not feasible for the $\text{TE}_{43,15}$ mode. Although this mode can be excited, maintaining wall loading limits would necessitate either reducing efficiency or output power. Alternatively, a higher mode, such as $\text{TE}_{52,18}$, could be explored to potentially reach output levels up to 1.5 MW. However, this mode presents additional challenges, including a higher risk of mode competition and a requirement for even tighter beam alignment, with a maximum allowable misalignment tolerance of only 0.3 mm. In addition, proper excitation of the $\text{TE}_{52,18}$ mode would require even stricter beam alignment tolerances, with the current maximum misalignment tolerance set at just 0.3 mm.

For the coaxial cavity, re-purposing an existing, proven design is under consideration. This cavity, which has already demonstrated reliable operation at 170 GHz [15], presents a cost-effective option by allowing reuse of many components with the added confidence in its proven functionality. The adaptation would involve tuning the electron beam and magnetic field for higher-frequency operation and integrating a new insert to support the new mode excitation. Specifically, the $\text{TE}_{48,26}$ is explored for operation at 238 GHz, which is capable of delivering output powers exceeding 1.5 MW, as shown in Figure 3.

Choosing not to repurpose an existing cavity but instead designing a new one makes the $\text{TE}_{49,29}$ mode a viable option, as suggested in [12]. This approach enables achieving even higher output power. Additionally, such a cavity has the

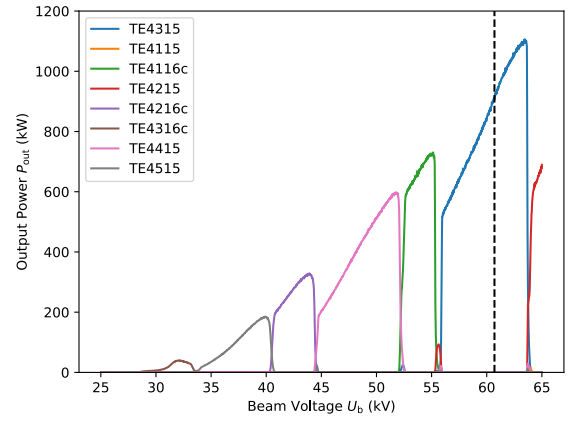


Fig. 2. Start-up scenario for the $\text{TE}_{43,15}$ hollow cavity, taking into account competing modes and realistic electron beam parameters. The black dashed line marks the point where the wall loading limit of 2 kW cm^{-2} is reached. The "c" following the mode denotes counter-rotation relative to the direction of electron beam rotation.

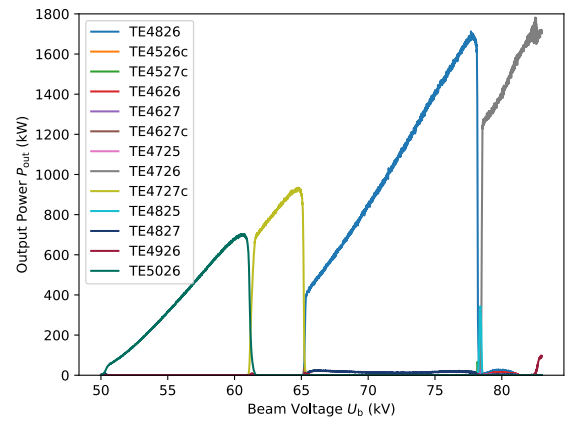


Fig. 3. Start-up scenario for the $\text{TE}_{48,26}$ coaxial cavity, taking into account competing modes and realistic electron beam parameters, similar to Figure 2

advantage of supporting operation at 170 GHz with the $\text{TE}_{35,21}$ mode and at 204 GHz with the $\text{TE}_{42,25}$ mode, considering the constraints imposed by the diamond window and the gyrotron launcher. Figure 4 illustrates a start-up simulation for a cavity specifically designed for these parameters. Table 1 summarizes the key operational parameters for the hollow and coaxial cavities under consideration.

B. Magnetron Injection Gun

Similar to the coaxial cavity, the triode MIG design with a 60 mm emitter radius [16] is being considered for reuse

Table 1. Parameters at the possible operation point considered for the simulations

	Hollow		Coaxial
Mode	$\text{TE}_{43,15}$	$\text{TE}_{48,26}$	$\text{TE}_{49,29}$
Frequency	236 GHz	237.2 GHz	237.5 GHz
Magnetic Field	9.165 T	9.55 T	9.58 T
Beam voltage	61 kV	77 kV	86 kV
Current	43 A	59 A	69 A
Output Power	0.9 MW	1.6 MW	2 MW
Thermal load	2 kW cm^{-2}	1.9 kW cm^{-2}	1.8 kW cm^{-2}
Efficiency	35%	37%	34%
Pitch factor	1.25	1.21	1.23

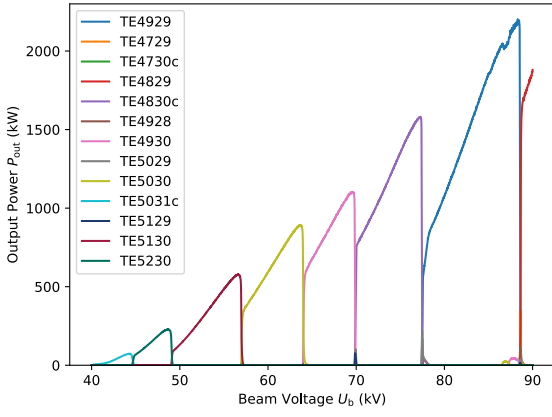


Fig. 4. Start-up scenario for the TE_{49,29} coaxial cavity, taking into account competing modes and realistic electron beam parameters, similar to Figure 2

Table 2. Simulation parameters for the triode MIG for TE_{43,15} and TE_{49,29}

	Hollow	Coaxial	Requirements
Acceleration Voltage	64 kV	89 kV	
Pitch factor	1.25	1.24	
Pitch factor spread	±5.2 %	±3.9 %	≤8 %
Beam radius	9.00 mm	10.24 mm	
Beam radius spread	±0.1 mm	±0.1 mm	$= \frac{\lambda}{6.2} \leq \frac{\lambda}{4}$

due to its established performance and reliability. The critical criteria for this are the tolerances, with the most important being the alpha spread (5 % to 8 %) and the beam radius spread (approximately $\lambda/4$ to $\lambda/5$). The gun setup has been simulated with the magnetic field profile of the 10.5 T super conducting gyrotron magnet.

Table 2 presents the simulated parameters for the triode MIG. The acceleration voltage represents the actual voltage that must be applied to the gun to achieve the desired beam voltage. In the triode configuration, the desired beam parameters at the cavity entrance can be reliably achieved for both the hollow and coaxial cavities. For the coaxial cavity, this is possible for both modes; however, only the TE_{49,29} mode is listed in this table.

IV. CONCLUSION AND OUTLOOK

Initial steps have been taken toward developing a gyrotron capable of operating at frequencies around 240 GHz, with the decision to pursue a coaxial gyrotron design incorporating a triode. This approach builds on proven designs, such as the 170 GHz cavity, aiming for high-power output and efficient operation at higher frequencies. Upcoming simulations will expand from the MIG to the beginning of the quasi-optical mode converter, offering a comprehensive assessment of integration and performance. To evaluate the influence of the coaxial insert, additional simulations and experimental studies are planned with the 170 GHz gyrotron, operating without the insert. Following these simulations, preparations will commence for experimental testing at the FULGOR facility, utilizing a state-of-the-art 10.5 T superconducting magnet.

REFERENCES

- [1] M. Thumm, "State-of-the-Art of High-Power Gyro-Devices - Update of Experimental Results 2023," Karlsruhe: KIT Scientific Publishing, 2024, p. 166. DOI: 10.5445/KSP/1000164947.
- [2] T. Rzesnicki, K. A. Avramidis, I. Chelis, *et al.*, "1.5 MW, 140 GHz Gyrotron for W7-X - development status and experimental results -," in *2022 47th International Conference on Infrared, Millimeter and Terahertz Waves (IRMMW-THz)*, 2022, pp. 1–2. DOI: 10.1109/IRMMW-THz50927.2022.9896025.
- [3] J. Jelonnek, G. Gantenbein, K. Hesch, *et al.*, "From series production of gyrotrons for W7-X towards EU-1 MW gyrotrons for ITER," in *19th IEEE Pulsed Power Conference (PPC), San Francisco, CA, USA, 16-21 June 2013*, 31.40.07; LK 01, Institute of Electrical and Electronics Engineers (IEEE), 2013, 1–6, ISBN: 978-1-4673-5168-3. DOI: 10.1109/PPC.2013.6627710.
- [4] T. Ruess, K. A. Avramidis, G. Gantenbein, *et al.*, "Theoretical Study on the Operation of the EU/KIT TE34,19-Mode Coaxial-Cavity Gyrotron at 170/204/238 GHz," *The European physical journal / Web of Conferences*, vol. 203, Article no: 04014, 2019, 31.03.02; LK 01, ISSN: 2100-014X. DOI: 10.1051/epjconf/201920304014.
- [5] G. Federici, W. Biel, M. Gilbert, R. Kemp, N. Taylor, and R. Wenninger, "European DEMO design strategy and consequences for materials," *Nuclear Fusion*, vol. 57, p. 092002, Sep. 2017. DOI: 10.1088/1741-4326/57/9/092002.
- [6] S. Kern, "Numerische Simulation der Gyrotron-Wechselwirkung in koaxialen Resonatoren," German, 31.04.02; LK 01, Ph.D. dissertation, 1996, 228 pp. DOI: 10.5445/IR/55396.
- [7] A. Leggieri, S. Alberti, K. Avramidis, *et al.*, "THALES TH1507 140 GHz 1 MW CW Gyrotron for W7-X Stellarator," Sep. 2019, pp. 1–3. DOI: 10.1109/IRMMW-THz.2019.8874589.
- [8] V. Myasnikov, M. Agapova, A. Kuftin, *et al.*, "New results of extra-powerful 1.5MW/170GHz gyrotron development," Sep. 2014, pp. 1–2. DOI: 10.1109/IRMMW-THz.2014.6956474.
- [9] R. Ikeda, T. Shinya, S. Yajima, *et al.*, "Multi-frequency, megawatt-power gyrotron to facilitate a wide range of operations at ITER," *Nuclear Fusion*, vol. 63, no. 6, p. 066028, 2023. DOI: 10.1088/1741-4326/accdeb. [Online]. Available: <https://dx.doi.org/10.1088/1741-4326/accdeb>.
- [10] P. C. Kalaria, "Feasibility and Operational Limits for a 236 GHz Hollow-Cavity Gyrotron for DEMO," Ph.D. dissertation, Karlsruhe, 2017, p. 270, ISBN: 978-3-7315-0717-8. DOI: 10.5445/KSP/1000073581.
- [11] E. Borie, "Review of gyrotron theory," Tech. Rep., 1991, 03.04.02; LK 01; KfK-4898 (August 91). DOI: 10.5445/IR/270031114.
- [12] J. Franck, "Systematic Study of Key Components for a Coaxial-Cavity Gyrotron for DEMO," Karlsruhe: KIT Scientific Publishing, 2017, p. 274, ISBN: 978-3-7315-0652-2. DOI: 10.5445/KSP/1000068000.
- [13] K. Avramidis, I. Pagonakis, C. Iatrou, and J. Vomvoridis, "EURIDICE: A code-package for gyrotron interaction simulations and cavity design," vol. 32, Sep. 2012. DOI: 10.1051/epjconf/20123204016.
- [14] S. Illy, J. Zhang, and J. Jelonnek, "Gyrotron electron gun and collector simulation with the ESRAY beam optics code," Apr. 2015, pp. 1–2. DOI: 10.1109/IVEC.2015.7223779.
- [15] Z. C. Ioannidis, T. Rzesnicki, K. A. Avramidis, *et al.*, "Operation of the Modular KIT 170 GHz – 2 MW Longer-Pulse Coaxial-Cavity Gyrotron with Pulses up to 50 ms," in *2020 45th International Conference on Infrared, Millimeter, and Terahertz Waves (IRMMW-THz)*, 2020, pp. 01–02. DOI: 10.1109/IRMMW-THz46771.2020.9370698.
- [16] I. G. Pagonakis, K. A. Avramidis, G. Gantenbein, *et al.*, "Triode magnetron injection gun for the KIT 2 MW 170 GHz coaxial cavity gyrotron," *Physics of plasmas*, vol. 27, no. 2, Article no: 023105, 2020, 31.03.02; LK 01, ISSN: 1070-664X, 1089-7674. DOI: 10.1063/1.5132615.